Cross-Linking in Adhesive Quinoproteins: Studies with Model Decapeptides†

Luis A. Burzio‡

College of Marine Studies, University of Delaware, Newark, Delaware 19916

J. Herbert Waite*

Marine Science Institute/MCDB Department, University of California, Santa Barbara, California 93106

Received February 2, 2000; Revised Manuscript Received May 10, 2000

ABSTRACT: *Mytilus edulis* foot protein-1 (mefp1) is a major component of the byssus, an adhesive holdfast in mussels. The recent report of 5,5′-di(dihydroxyphenyl-L-alanine) (diDOPA) cross-links in byssus [McDowell et al. (1999) *J. Biol. Chem. 274,* 20293] has raised questions about the relationship of these to mefp1. About 80% of the primary structure of mefp1 consists of a tandemly repeated consensus sequence Ala[1]-Lys[2]-Pro[3]-Ser[4]-Tyr[5]-Pro[6]-Pro[7]-Thr[8]-Tyr[9]-Lys[10] with varying degrees of posttranslational hydroxylation to hydroxyprolines in positions 3, 6, and 7 and to DOPA in positions 5 and 9. Six natural or synthetic variants of this decapeptide were subjected to oxidation by tyrosinase or periodate. DOPA is the only residue to suffer losses in all oxidized peptides. Moreover, using MALDI TOF mass spectrometry, oxidized decapeptides all showed evidence of multimer formation and a mass loss of 6 Da per coupled pair of peptides. Multimer formation was inhibited by addition of DOPA-like *o*-diphenols, but addition of simple amines such as free Lys had no effect. The results are consistent with aryloxy coupling to diDOPA followed by reoxidation to diDOPA quinone. There are subtle but noteworthy variations, however, in multimer formation among the peptide congeners. Decapeptides with Pro[3] modified to *trans*-4-hydroxyproline do not form multimers beyond dimers; they also exhibit significant Lys losses following oxidation of DOPA. Moreover, in Ala-Lys-Hyp-Ser-Tyr-DiHyp-Hyp-Thr-DOPA-Lys, Tyr appears to be protected from oxidation by tyrosinase.

Blue mussels lead sedentary lives in the "fast lane" of ocean habitats where they withstand water flow velocities in excess of 10 m s^{-1} (*1*). Dislodgment is prevented by adopting a streamlined shape and by secreting a surface-bonding structure known as the byssus. The byssal proteins, like other structural adhesives, must fulfill two prerequisites to provide mussels with adequate attachment strength: strong interfacial coupling and structural cohesion (*2*). How these prerequisites are achieved is of paramount importance for mussel survival and is of interest to biomimetic engineering (*3*). Recent solid-state ^{13}C NMR analysis of byssal attachment plaques has suggested that structural cohesion or "cure" develops through the formation of 5,5′-di(3, 4-dihydroxyphenyl-L-alanine) or diDOPA cross-links whose density in byssus appears to be correlated to water flow (*4*).

In all likelihood, the diDOPA cross-links are formed from peptidyl DOPA residues which are present in at least eight byssal precursor proteins (*5*). Although *o*-diphenolic-derived *o*-quinones are not known for their reactive specificity, under certain defined reaction conditions phenolic coupling can be the preferred reaction pathway (*6*, *7*). One byssal precursor, *Mytilus edulis* foot protein-1 (mefp1), has a molecular weight of 110 000 (*8*) and consists largely of tandemly repeated DOPA-containing decapeptides: Ala-Lys-Pro-Ser-Tyr-Di-Hyp-Hyp-Thr-DOPA-Lys, where DiHyp and Hyp in positions 6 and 7 denote *trans*-2,3-*cis*-3,4-dihydroxyproline and *trans*-4-hydroxyproline, respectively (*9*, *10*). Mefp1 polymerizes in vitro at pH 7−8 upon oxidation by peroxide, periodate, or various phenolases (*11*−*14*). Oxidation is accompanied by the formation of multiple quinone functionalities, i.e., a quinoprotein, an increase in mass, and, after acid hydrolysis, a decrease in detectable DOPA (*15*).

In this study, the chemical effects of oxidation on mefp1-derived or -inspired decapeptide sequences in vitro were investigated. Our results show that such peptides readily form multimers and are consistent with the formation of diDOPA cross-links. That mefp1 cross-linking contributes to the cohesiveness of byssus thus seems a reasonable assumption.

EXPERIMENTAL PROCEDURES

Preparation of Decapeptides. Synthetic adhesive decapeptide was purchased from Sigma and hydroxylated according to a published procedure (*16*). Briefly, decapeptide was dissolved in 4 mL of 100 mM phosphate, pH 7.5, with 25 mM ascorbic acid at room temperature with constant stirring and aeration. Tyrosinase (3400 units mg^{-1}; Sigma) was added to start the reaction and allowed to proceed for 60 min. For tyrosine monophenolase activity, a unit is defined as a change of 0.01 min^{-1} mL^{-1} at 280 nm with L-tyrosine as the substrate. The reaction was terminated by addition of 25 μL of 6 N HCl/mL.

† Supported by grants from the Biomaterials Program at the NIDCFR (DE10042) and the Office of Naval Research (N00014-99-1-0774).

* Corresponding author. Fax: (805) 893-7998. E-mail: waite@lifesci.ucsb.edu.

‡ Present address: Surgical Sealants, Inc., Woburn, MA 01801.

10.1021/bi0002434 CCC: $19.00
Published on Web 08/17/2000

The differentially hydroxylated decapeptides were separated by reversed-phase HPLC on a C-8 column (Brownlee RP-300) using the following gradient made by mixing 0.1% (v/v) trifluoroacetic acid (TFA)[1] in water with 0.1% (v/v) TFA in acetonitrile (B): 0−5% B in 5 min, to 15% B in 50 min, and, finally, 100% B at 60 min. Collected fractions (1 mL each) were lyophilized and reconstituted in water. The extent and location of hydroxylation were determined by MALDI TOF mass spectrometry and microsequencing, respectively.

Mefp1-derived decapeptides were obtained by trypsinization. Mefp1 was purified from mussel feet obtained by the kilogram from Northeast Transport (Union, ME) (*17*). HPLC-purified mefp1 (∼5 mg) was dissolved in 4 mL of 100 mM Tris-HCl at pH 7.0 and 0.02 mM $CaCl_2$. Trypsin was added at a weight ratio of 1:20 (trypsin:mefp1), and the digestion was stirred for 4 h. The reaction was stopped with 100 μL of 6 N HCl. Decapeptide variants were separated by C-8 reversed-phase HPLC (Brownlee RP-300) using a water: acetonitrile (B) gradient of 0−5% B in 5 min, to 10% at 45 min, and 100% B at 65 min (*17*). Collected fractions (1 mL each) were freeze-dried. Decapeptides were characterized by MALDI TOF mass spectrometry and microsequencing.

Peptide Oxidation. Sodium periodate (Sigma), mushroom tyrosinase (Sigma; SA = 3400 units mg^{-1}, where each unit equals a difference in absorbance at 265 nm of 0.001 min^{-1} mL^{-1} at pH 6.5 at 25 °C in a reaction mix containing either L-DOPA or catechol and L-ascorbic acid), and byssal catechol oxidase [*15*; SA = 7 mmol min^{-1} (mg of protein)$^{-1}$] were used as oxidants. For peptides cross-linked with tyrosinase or byssal catechol oxidase, the reaction was begun by adding 0.05 μg of enzyme/mL at a 50:1 peptide:enzyme weight ratio in 50 mM Tris, pH 7.5, with stirring at room temperature. Periodate oxidation was also done in Tris at an equimolar periodate:DOPA molar ratio. UV−vis absorbance was measured on a Hewlett-Packard diode array spectrophotometer (HP model 8453) equipped with interface 35900E and ChemStation software. Spectra were taken at 5 min intervals for a total 30 min reaction time.

Chemical Characterization. Mass spectrometry was done using a PE Biosystems Voyager DE instrument with delayed extraction. Matrix (α-cyano-3-hydroxycinnamic acid) was prepared as a saturated solution in 1:1 (v/v) water:acetonitrile with 0.1% TFA. All samples were run in linear mode with 20 kV accelerating voltage, 18.6 kV grid voltage, and 15 V guide wire voltage. The typical laser power setting was 1800. Microsequencing was done with a Porton P-2090 sequencer (Beckman Instruments, Fullerton) with DOPA and *trans*-4-hydroxyproline standards (*17*). Peptide samples were hydrolyzed in vacuo using 6 N HCl with 10% (v/v) TFA and 5% (v/v) phenol for 30 min at 156 °C (*18*). Hydrolysates were flash evaporated at 55 °C and washed with 200 μL each of deionized water, methanol, and deionized water. The final residue was resuspended in 40−100 μL of sample buffer prior to loading and running on a Beckman 6300 autoanalyzer, which has a dual wavelength ninhydrin-based detection system (*17*). Dimers formed from the oxidation of YY* (Table 1) were purified by C-8 HPLC using the following gradient: 0−5% B in 5 min, to 20% at 55 min, followed by a 100% wash for 10 min. The dimer eluted at about 45 min or around 13% B.

[1] Abbreviations: MALDI TOF, matrix-assisted laser desorption ionization with time of flight; SA, specific activity; TFA, trifluoroacetic acid.

Table 1: Sequences and *m/z* Values for Mefp1-Inspired or -Derived Decapeptides Used in This Study[a]

	shorthand	*m/z* (calcd)	*m/z* (obsd)
natural peptides			
AK**P**SY***P****TY*K	P*Y*Y*	1248.35	1248.3
AK**P**SY**P*****P**TY*K	P*YY*	1232.35	1232.3
AKPSY***P*****P**TY*K	PY*Y*	1232.35	1232.3
AKPSY**P*****P**TY*K	PYY*	1216.35	1216.3
synthetic peptides			
AKPSY***PP**TY*K	Y*Y*	1216.35	1216.3
AKPSY**PP**TY*K	YY*	1200.35	1200.3
AKPSY**PP**TYK	YY	1184.35	1184.3

[a] **P** = *trans*-4-hydroxyproline; **P*** = *trans*-2,3-*cis*-3,4-dihydroxyproline; Y* = 3,4-dihydroxyphenylalanine.

RESULTS

We have investigated the enzymatic and periodate-based oxidation of decapeptide variants related to or derived from the marine adhesive protein mefp1. The variants are of two types: "natural", as derived by trypsin digestion of mefp1, and "synthetic" (Table 1), in which Tyr residues in positions 5 and 9 are differentially hydroxylated using an enzymatic method and purified by C-8 HPLC (Figure 1). Although both types exhibit similar hydroxylation patterns, they differ in one respect: natural peptides all have *trans*-2,3-*cis*-3,4-dihydroxyproline in position 6 while the synthetics have *trans*-4-hydroxyproline there. Short-hand nomenclature for the peptides reflects only the variable positions: thus, P*Y*Y*, P*YY*, PY*Y*, and PYY* describe the natural peptides that vary at positions 3, 5, and 9 of the decapeptide, while the synthetics, YY* and Y*Y*, vary only at positions 5 and 9 (see Table 1).

UV−vis spectra of periodate oxidized and enzymatically oxidized decapeptides are exhibited in Figure 2 and show broad absorbance changes over time. While similarities exist, none of these changes can be unequivocally associated with the absorbance spectra for several well-characterized oxidation products on the basis of the model compounds, 4-methyl- or 4-ethylcatechol (Figure 3). Intermediates detected at 395−400 nm (e.g., Figure 2C) coincide with simple *o*-quinones (**II**) formed from catechols (**I**). The subsequent absorbance shifts to higher wavelengths, for example, 410−460 nm, compare favorably with the λ_{max} of coupled 6,6′-dicatechols (**IIIa**). Absorbance maxima above 500 nm, which are characteristic for model Michael additions (**IV**), were not observed with tyrosinase or periodate as oxidant. While both tyrosinase-oxidized P*Y*Y* and Y*Y* have absorbance increases at similar wavelengths, they differ in details: P*Y*Y* shows a maximum at 410 nm, whereas in Y*Y*, the maximum is shifted to 425 nm (Figure 2A,B). With periodate as oxidant, the maxima for YY* and Y*Y* are similar, though in YY* an intermediate is evident (395 nm), and the higher maximum is shifted up to 462 nm (Figure 2C,D).

Amino acid analyses of hydrolyzed aliquots of oxidized and polymerized decapeptides all show two general trends: a decrease of DOPA to near-zero levels and a partial decrease in Tyr when it is present (except in P*YY*) (Table 2).

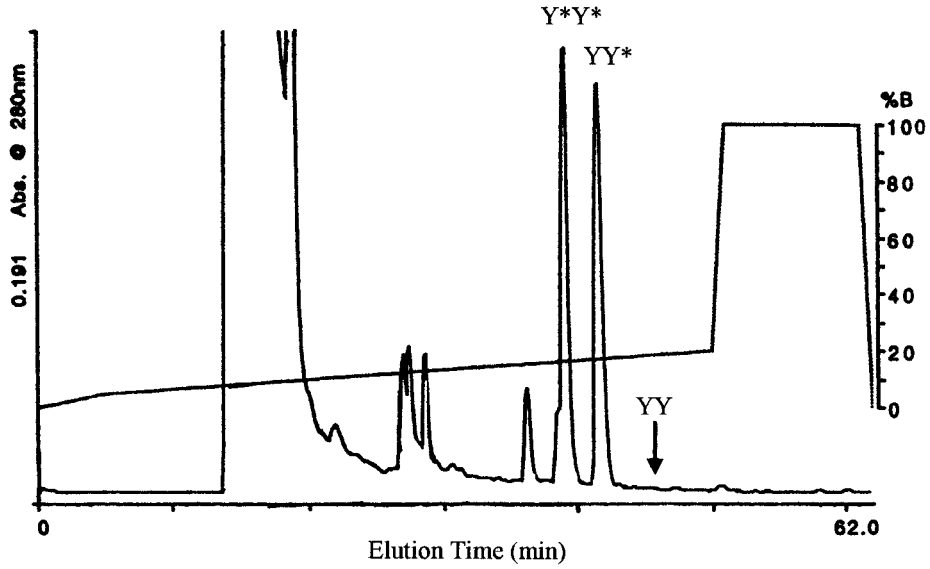

FIGURE 1: Reversed-phase HPLC elution profile of enzymatically hydroxylated synthetic decapeptides. Hydroxylation was carried out at a 100:1 (w/w) protein to tyrosinase ratio using conditions specified in Experimental Procedures. Peaks represent decapeptide with DOPA in the 5 and 9 positions (Y*Y*) and decapeptide with DOPA in the 9 position (YY*), respectively. Peptide without DOPA (YY) was the starting material. The elution gradient was acetonitrile (% B) with a flow rate of 1.0 mL/min. Absorbance was measured at 280 nm.

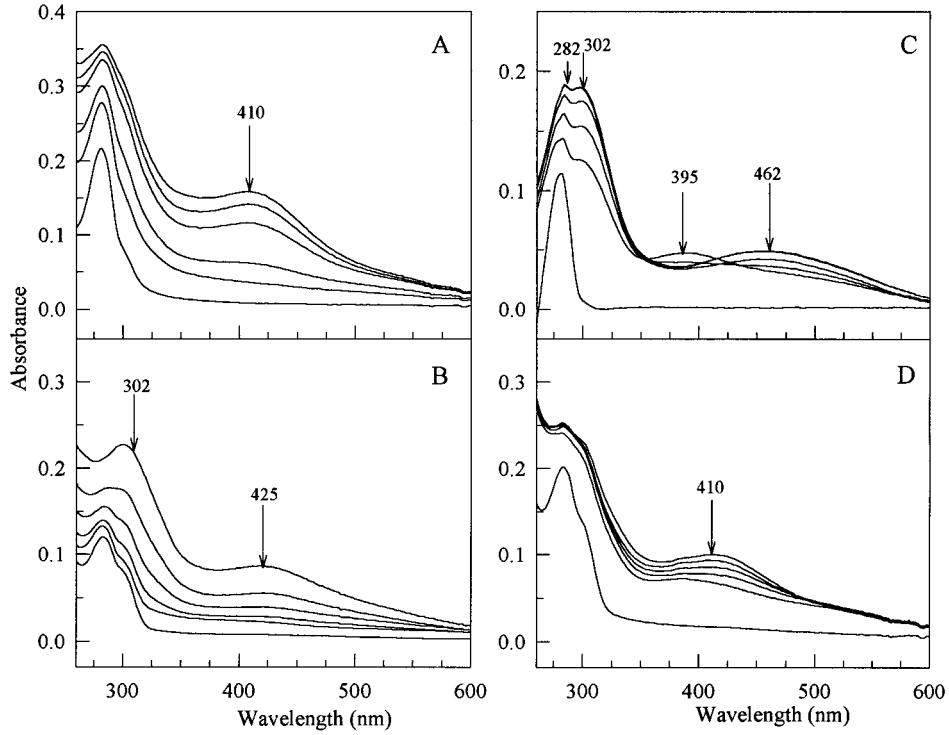

FIGURE 2: UV−vis absorbance properties of oxidized decapeptides in 50 mM Tris at pH 7.5 and 25 °C. Panels A and B represent peptides P*Y*Y* and Y*Y* oxidized by tyrosinase (50:1 substrate:enzyme weight ratio), while panels C and D are YY* and Y*Y* oxidized by periodate (equimolar with peptide DOPA concentrations). All oxidations were scanned at intervals of 0, 5, 15, 30, 60, and 120 min using tyrosinase and 0, 0.5, 1, 2, 5, and 15 min for periodate. Spectrum A for oxidized P*Y*Y* is typical for the other mefp1-derived variants.

Curiously, there are also significant Lys losses (30−50%) in peptides P*Y*Y* and P*YY*. In contrast, Lys is unaffected in PY*Y*, in PYY*, and in the synthetic decapeptides.

MALDI TOF mass spectrometry of oxidized natural and synthetic decapeptides (Figures 4 and 5) shows clear evidence of multimer formation up to 4X although it can go as high as 8X (Figure 4B). Curiously, in P*Y*Y* and P*YY*, multimers do not exceed dimer formation. Multimer formation occurs regardless of the oxidant used, e.g., periodate, byssal catechol oxidase, or tyrosinase (Figures 4B and 5A). In general, the mass (m_n) of the prominent peak in each multimer cluster is related to the monomer mass (m_1) by

$$m_n = nm_1 - 2m_H - 2^{n-1}m_H$$

where n is equal to the number of decapeptides coupled and m_H is the mass of a hydrogen atom. For example, the major peak in the dimer ($[M + H]^+ = 2392.9$) formed by periodate

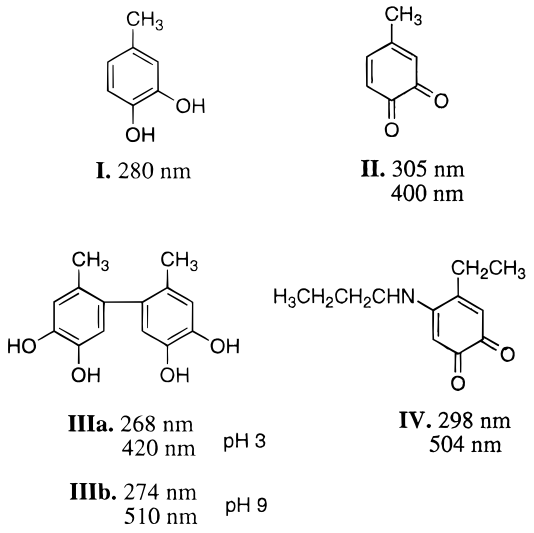

FIGURE 3: UV−vis absorbance maxima of model catechols, quinones, and derived cross-links. References for compounds **I**−**V** are as follows: **I** (*33*), **II** (*33*), **IIIa,b** (*7*), and **IV** (*24*).

Table 2: Amino Acid Analysis of Decapeptides before and 15 min after Tyrosinase Addition (Peptide:Enzyme Weight Ratio, 50:1)[a]

	fraction remaining for peptide					
residue	YY*	Y*Y*	P*Y*Y*	P*YY*	PY*Y*	PYY*
Ala	1	1	1	1	1	1
Ser	1	1	1	1	1	1
Thr	1	1	1	1	1	1
Lys	1	1	0.69	0.47	1	1
Pro	1	1	−	−	1	1
Hyp	1	1	1	1	1	1
DiHyp	−	−	1	1	1	1
DOPA	0.10	0.12	0.14	0.01	0.14	0.01
Tyr	0.40	−	−	0.94	−	0.40

[a] All peptide samples were hydrolyzed prior to analysis. Data are given as fraction remaining or the amount detected after 15 min relative to the amount present at time 0. Dashes (−) are used to indicate where certain residues are absent in some peptides. Variance ±10%.

oxidation of YY* is about 6 Da lower than the calculated 2 × 1199.3 + m_H. A larger peak, about 24 Da higher than the calculated dimer mass and 32 Da higher than the observed peak at 2392.9, may correspond to the addition of two H_2-Os to the DOPA-derived quinones. A smaller peak, at 24 Da lower than the calculated mass of n × monomers, is also detected (Figure 5B). Adjusting for the 6 Da loss already described, this is equivalent to the loss of one water (18 Da). The sequence of the YY* dimer as determined by automated Edman degradation exhibits identity with that of the monomer excepting a complete loss of detectable DOPA in position 9 (Table 3).

Addition of free glycine, lysine, or tyrosine to the oxidized decapeptides in 10× molar excess does not inhibit multimer formation but rather tends to spread out each multimeric peak in proportion to the mass of the added amino acid (Figure 6). *o*-Diphenol addition, in contrast, completely eliminates multimer formation. There is, however, a strong tendency for the diphenols to couple multiple times to the oxidized decapeptides. As many as 5−6 mol of 4-methylcatechol or *N*-acetyl-DOPA-amide can couple, for example, to each mole of synthetic peptide Y*Y* (Figure 7). We suggest that this is by aryloxy coupling to the peptidyl DOPA side chain as well as chain propagation of the coupled *o*-diphenols.

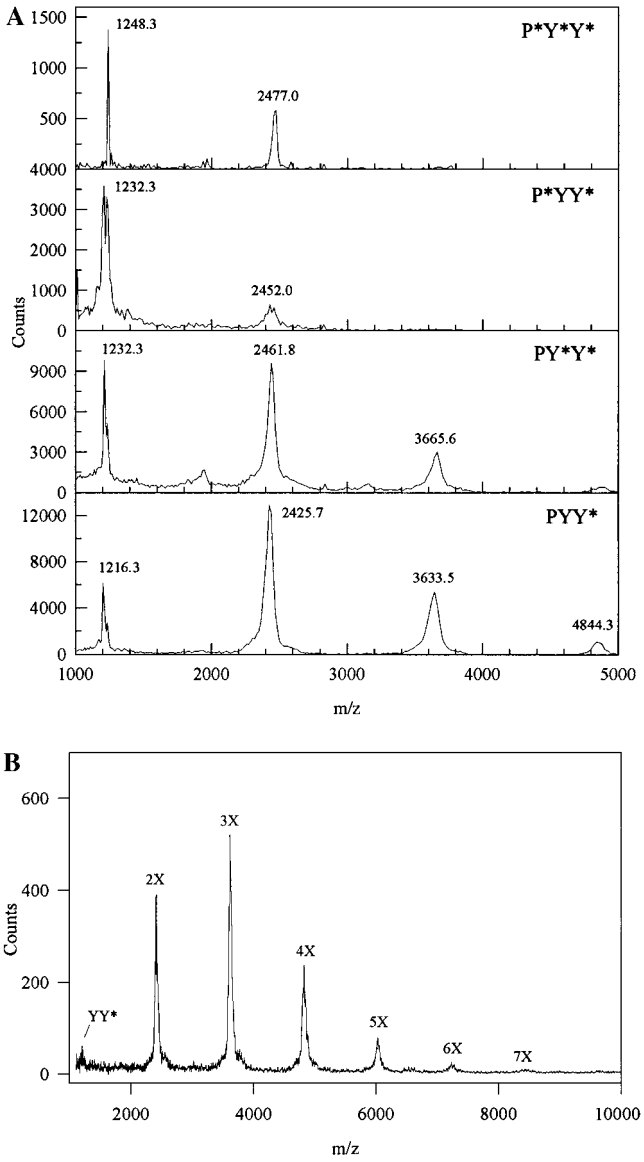

FIGURE 4: MALDI TOF mass spectra of decapeptide variants cross-linked with tyrosinase (A) and byssal catechol oxidase (B) at a 50:1 peptide YY*:enzyme weight ratio. Spectra were taken after a 30 min reaction time.

DISCUSSION

DOPA-containing peptides modeled after or derived from the consensus decapeptide repeats of mefp1 are readily oxidized to quinopeptides by tyrosinase or oxidants such as periodate. These quinopeptides undergo cross-linking detectable as decapeptide multimers by mass spectrometry. Tyrosinase-catalyzed oxidation of Tyr residues in various proteins has been an established technique in protein biochemistry and is known to involve a transient DOPA intermediate before the quinone product (*19*). The reactions following quinone formation, however, particularly the nature of quinone involvement in protein cross-linking, have been in dispute for many years.

There are two schools of thought regarding the interaction of *o*-quinone with proteins: (A) aryl−alkylamine addition and (B) aryloxy radical coupling. The first is usually based on Schiff base substitution and/or Michael-type addition reactions, i.e., nucleophilic attack of the β-carbon of an α,β-unsaturated *o*-quinone. Such a mechanism was initially

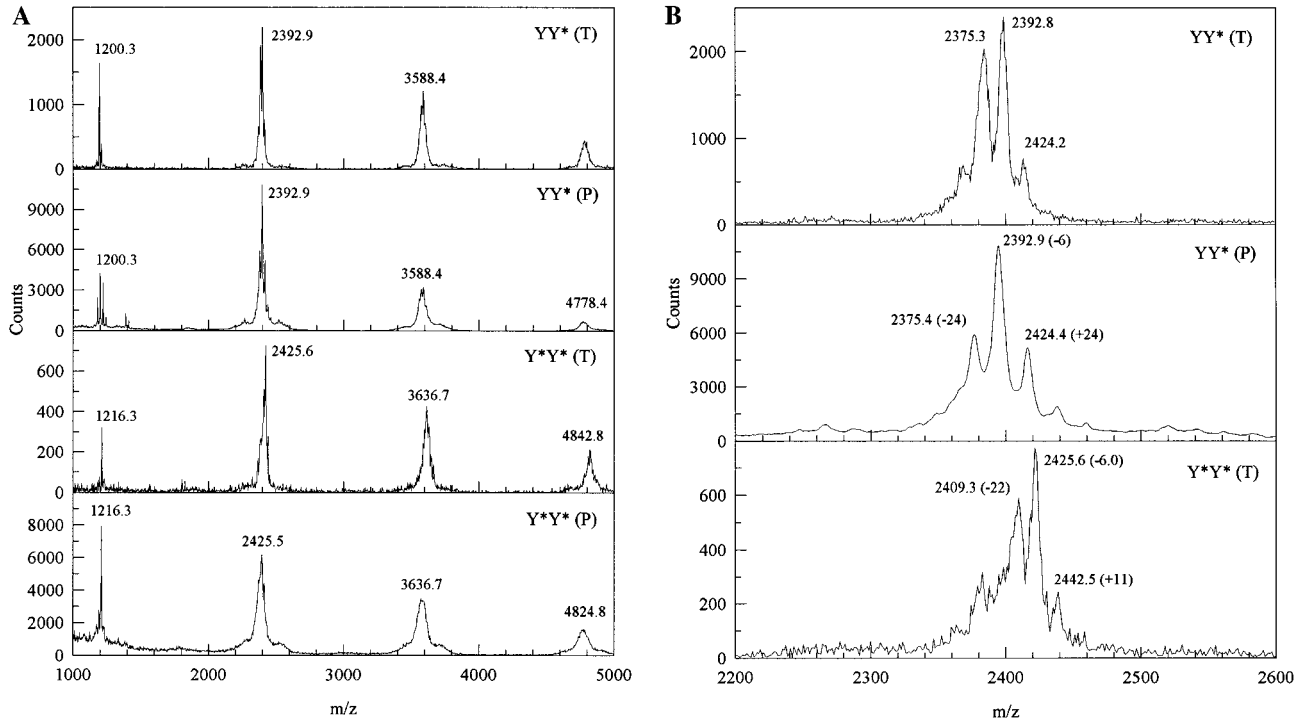

FIGURE 5: (A) MALDI TOF mass spectra of the synthetic peptides YY* and Y*Y* cross-linked with tyrosinase at a 50:1 weight ratio or a periodate:DOPA molar ratio of 1:1. Spectra were obtained after a 30 min reaction time. (B) Expanded view of the dimer (2X) peak from the previous spectra. Observed *m*/*z* values for the YY* dimer are the same for both the tyrosinase (T) and periodate (P) treatments. Parenthetical numbers correspond to the mass differences between the observed masses and the calculated sum of two monomer masses.

Table 3: Automated Edman Degradation of Approximately Equal Amounts of the YY* Monomer Compared with Dimer Formed by Tyrosinase Oxidation

		yield (pmol)	
cycle	amino acid	monomer	dimer
1	Ala	250	230
2	Lys	192	181
3	Pro	187	193
4	Ser[a]	106	98
5	Tyr	170	162
6	Hyp[b]	163	158
7	Hyp[b]	175	169
8	Thr	68	71
9	DOPA	178	
10	Lys	40	40

[a] Combines peak areas for PTH-Ser and PTH-dehydroalanine. [b] Combines peak areas for PTH-hydroxyproline and PTH-dehydroproline.

demonstrated in vitro with *o*-quinone and aniline (*20*) and later corroborated in at least three biochemically significant reactions: (1) side-chain condensation in DOPA quinone to form DOPA chrome and melanin (*21*), (2) adduct formation between *o*-quinone and nucleophilic amines such as proline (*22*) and histidine (*23*), and (3) nucleophilic attack of DOPA quinone by a lysyl residue near the active site of lysyl oxidase (*24*). Despite the very high levels of lysine in mefp1, for example, nucleophilic additions involving lysine and quinones have eluded detection in mussel byssus as well as related "quinone-tanned" proteins (*25*, *26*).

Aryloxy radical formation can occur when phenolic or diphenolic groups undergo one-electron oxidations. The aryloxy or semiquinone free radicals can then couple to form covalent aryl−aryl or aryl−ether bonds. Such bonds are common in peroxidase-catalyzed oxidations of Tyr-containing proteins (*26*) and in lignin (*27*). Coupled diDOPA cross-links were recently detected in mussel byssus (*4*).

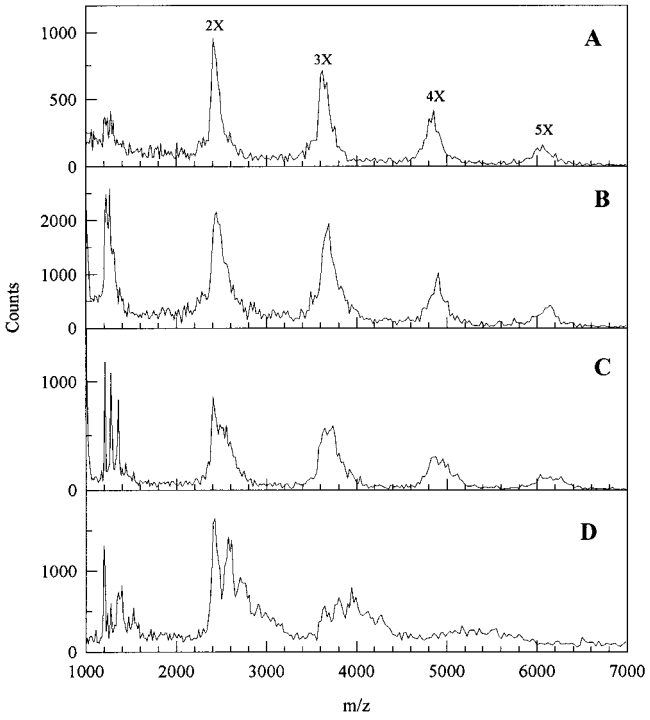

FIGURE 6: MALDI TOF mass spectrometry of the tyrosinase-catalyzed polymerization of Y*Y* (A) in the presence of a 10-fold molar excess of glycine (B), lysine (C), and tyrosine (D). All spectra were taken after a 60 min incubation period.

Since byssus contains many different proteins, it is important to determine which ones are coupled by diDOPA cross-links and what role, if any, Lys plays in cross-linking. Lys residues are clearly chemically reactive in two mefp1-derived decapeptides, P*YY* and P*YY*, as shown by losses evident by amino acid analysis. But is this reactivity

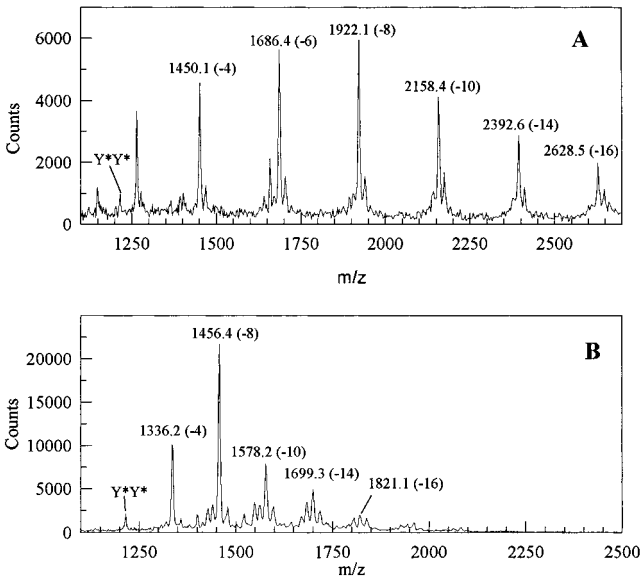

FIGURE 7: MALDI TOF spectra of Y*Y* multimer inhibition by (A) *N*-acetyl-DOPA-amide (mass 238) and (B) 4-methylcatechol (mass 124) using a 10-fold molar excess. Spectra were taken after a 60 min incubation period using a peptide:tyrosinase weight ratio of 50:1. Numbers above peaks indicate the *m*/*z*; those in parentheses, the $\Delta m/z$ between the theoretical and observed mass of the peptide with one, two, three, four, and five molecules of each catechol, respectively. The peak at *m*/*z* 48 Da higher than the monomer in figure 6A is an impurity.

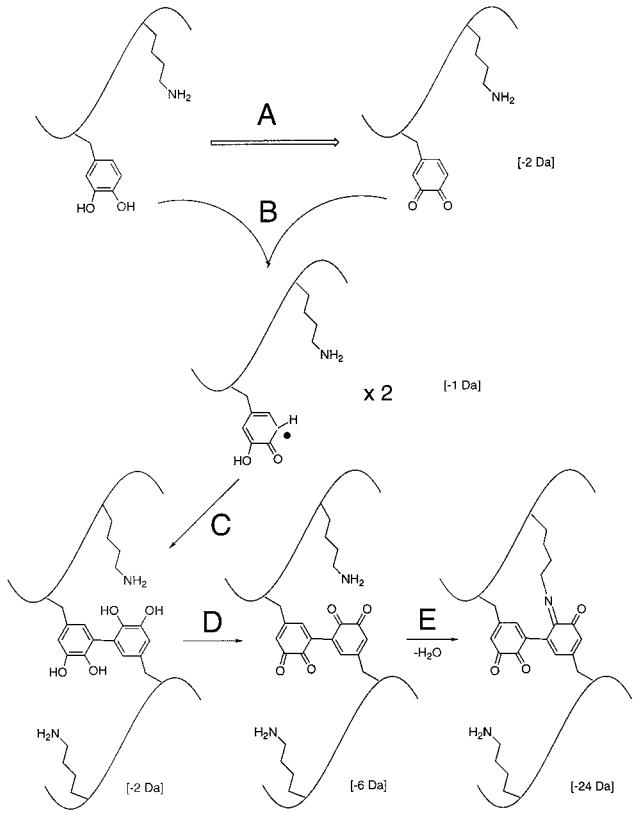

FIGURE 8: Proposed reaction pathway for cross-linking in oxidized mefp1-derived decapeptides. Steps: (A) catechol oxidase or tyrosinase-catalyzed oxidation requiring O_2; (B) reverse dismutation to aryloxy free radicals; (C) aryloxy free radical coupling; (D) reoxidation of coupled diphenols that is probably enzyme-catalyzed with one ring oxidized as a likely intermediate; (E) intramolecular Schiff base reaction with lysine.

necessarily involved with cross-linking? A decrease of $\Delta m/z = -2$, -4, or -6 can be reconciled with either aryloxy coupling or Michael addition reactions (Figure 3), followed by oxidation of one or both rings to quinones. That Lys is not necessary for intermolecular cross-linking of most decapeptides, however, is most clearly shown by MALDI TOF analysis of multimer formation in the presence of large excesses of the free amino acids, lysine, glycine, or tyrosine (Figure 7). All of these have an α-amino group that might inhibit multimer formation by competing with peptidyl lysine. Multimer formation in oxidized decapeptides, however, is unimpeded in the presence of the amino acids, although each peak is broadened by adduct formation. We propose that while not directly involved in cross-linking of decapeptides, Lys residues may participate in intramolecular side reactions with the cross-links formed. The observed satellite peak at $\Delta m/z = -18$ in the dimer of peptide YY* suggests a Schiff base addition between a Lys residue and the cross-link (Figure 6). This needs to be confirmed, but it is commonplace in the bioorganic chemistry of quinones (*29*). The fact that amino acid analyses of most oxidized decapeptides did not show losses in Lys may owe to the lability of Schiff base and even Michael additions to acid hydrolysis (*30*).

The loss in detectable DOPA is the only universally consistent change accompanying oxidation of the decapeptides. This loss could be attributed entirely to the formation of DOPA quinone or to the formation of DOPA-derived cross-links. The decapeptide multimers detected by MALDI TOF mass spectrometry argue cogently for cross-link formation. Not only do multimers (dimers to hexamers) form within minutes of tyrosinase or periodate addition, but the $\Delta m/z$ of -6 in dimerization is consistent with ring coupling ($\Delta m/z = -2$), followed by oxidation of each diphenolic ring to quinone ($\Delta m/z = -2$ per ring) (Figure 7). The dimer of YY* was isolated, and upon sequencing, only the DOPA residues in position 9 were found to be missing, suggesting these to be modified. Finally, the complete inhibition of multimer formation by low molecular weight analogues of peptidyl DOPA such as 4-methylcatechol and *N*-acetyl-DOPA-amide suggests that they compete effectively with cross-linking sites. Both compounds added multiply to the decapeptides, perhaps by phenol coupling ($\Delta m/z = -2$) followed by oxidation to quinone ($\Delta m/z = -2$ per ring). The fact that up to six such adducts could be observed for each oxidized decapeptide suggests a very high coupling capacity.

It would appear that while posttranslational hydroxylation of Pro-3 in the decapeptides does influence the cross-linking behavior of specific peptides, the dihydroxylation of Pro-6 does not. Compare, for example, P*YY* and P*Y*Y* with all others. Only those peptides with Hyp in position 3 show impeded multimer formation beyond the dimer, increased Lys reactivity, and decreased Tyr reactivity. In contrast, a comparison of the peptide pair PYY* and PY*Y* with YY* and Y*Y* (in which the latter pair lacks the second hydroxylation on Pro-6) reveals no difference in cross-linking behavior.

In summary, DOPA-containing decapeptides based on the sequence of mefp1 are shown to be effectively cross-linked following oxidation to quinopeptides. Although the mechanism of cross-link formation is not known, reverse dismutation of the quinone with DOPA to produce two aryloxy

free radicals or semiquinones that couple to form a diDOPA is suggested and corroborated by ESR detection of free radicals during tyrosinase action (*31*, *32*) (Figure 8). The specific aryl carbons coupled cannot be ascertained from the present data, but 5,5′-diDOPA coupling in byssus was predicted by solid-state ^{13}C NMR data (*4*).

ACKNOWLEDGMENT

We thank Dr. G. Nicol for guidance in mass spectrometry and helpful discussions. Dr. L. Rzepecki synthesized and generously donated *N*-acetyl-DOPA-amide.

REFERENCES

1. Bell, E. C., and Gosline, J. M. (1997) *Mar. Biol. Ecol. Prog. Ser. 159*, 197−208.
2. Schonhorn, H. (1981) in *Adhesion in Cellulosic and Wood-based Composites* (Oliver, J. F., Ed.) pp 91−111, Plenum Publishing Corp., New York.
3. Deming, T. J. (1999) *Curr. Opin. Chem. Biol. 3*, 100−105.
4. McDowell, L. M., Burzio, L. A., Waite, J. H., and Schaefer, J. (1999) *J. Biol. Chem. 274*, 20293−20295.
5. Waite, J. H. (1997) *J. Adhes. Soc. Jpn. 33*, 186−193.
6. Brown, B. R. (1967) in *Oxidative Coupling of Phenols* (Taylor, W. I., and Battersby, A. R., Eds.) Chapter 4, pp 167−201, Dekker Inc., New York.
7. Andersen, S. O., Jacobsen, J. P., Bojesen, G., and Roepstorff, P. (1992) *Biochim. Biophys. Acta 1118*, 134−138.
8. Deacon, M. P., Davis, S. S., Waite, J. H., and Harding, S. E. (1998) *Biochemistry 37*, 14108−14112.
9. Taylor, S. W., Waite, J. H., Ross, M. M., Shabanowitz, J., and Hunt, D. F. (1994) *J. Am. Chem. Soc. 116*, 10803−10804.
10. Laursen, R. (1992) *Results Probl. Cell Differ. 19*, 52−72.
11. Filpula, D. R., Lee, S. M., Link, R. P., Strausberg, S. L., and Strausberg, R. L. (1990) *Biotechnol. Prog. 6*, 171−177.
12. Hansen, D. C., Corcoran, S. G., and Waite, J. H. (1998) *Langmuir 14*, 743−746.
13. Yamamoto, H., and Tatehata, H. (1995) *J. Mar. Biotechnol. 2*, 95−100.
14. Kitamura, M., Kawakami, K., Nakamura, N., Tsumoto, K., Uchiyama, H., Ueda, Y., Kumagai, I., and Nakaya, T. (1999) *J. Polym. Sci. 37A*, 729−736.
15. Burzio, L. A. (1999) Ph.D. Thesis, University of Delaware, Newark, DE.
16. Marumo, K., and Waite, J. H. (1986) *Biochim. Biophys. Acta 872*, 98−103.
17. Waite, J. H. (1995) *Methods Enzymol. 258*, 1−19.
18. Tsugita, A., Uchida, T., Mewes, H. W., and Ataka, T. (1987) *J. Biochem. 102*, 1595−1597.
19. Sizer, I. (1953) *Adv. Enzymol. 14*, 129−171.
20. Hackman, R. H., and Todd, A. R. (1953) *Biochem. J. 55*, 631−637.
21. Mason, H. S. (1948) *J. Biol. Chem. 172*, 83−99.
22. Mason, H. S., and Peterson, E. W. (1955) *Biochim. Biophys. Acta 111*, 134−146.
23. Xu, R., Huang, X., Hopkins, T. L., and Kramer, K. J. (1997) *Insect Biochem. Mol. Biol. 27*, 101−108.
24. Wang, S. X., Mure, M., Medzihradsky, K. F., Burlingame, A. L., Brown, D. E., Dooley, D. M., Smith, A. J., Kagan, H. K., and Klinman, J. P. (1996) *Science 273*, 1078−1084.
25. Holl, S. M., Hansen, D. C., Waite, J. H., and Schaefer, J. (1993) *Arch. Biochem. Biophys. 302*, 255−258.
26. Klug, C. A., Burzio, L. A., Waite, J. H., and Schaefer, J. (1996) *Arch. Biochem. Biophys. 333*, 221−224.
27. Michon, T., Chenu, M., Kellershon, N., Desmadril, M., and Gueguen, J. (1997) *Biopolymers 36*, 8504−8513.
28. Zimmermann, W. (1989) *Chimia 43*, 396−403.
29. Wilmot, C. M., Hajdu, J., McPherson, M. J., Knowles, P. F., and Phillips, S. E. V. (1999) *Science 286*, 1724−1728.
30. Benavente, M. G., and Truscott, R. J. W. (1991) *Arch. Biochem. Biophys. 290*, 451−457.
31. Mason, H. S., Spencer, E., and Yamazaki, I. (1961) *Biochem. Biophys. Res. Commun. 4*, 236−238.
32. Koga, S., Nakano, S., and Tero-Kubota, S. (1992) *Arch. Biochem. Biophys. 292*, 570−575.
33. Waite, J. H. (1976) *Anal. Biochem. 75*, 211−218.

BI0002434